JOURNAL OF GEOPHYSICAL RESEARCH, VOL. 113, A02204, doi:10.1029/2007JA012466, 2008

Extended SuperDARN and IMAGE observations for northward IMF: Evidence for dual lobe reconnection

M. F. Marcucci,[1] I. Coco,[1] D. Ambrosino,[1] E. Amata,[1] S. E. Milan,[2] M. B. Bavassano Cattaneo,[1] and A. Retinò[3]

Received 12 April 2007; revised 11 September 2007; accepted 9 October 2007; published 6 February 2008.

[1] We present observations of ionospheric convection in the Northern Hemisphere made by the SuperDARN radar network during a 3 h period on 3 December 2001. The interplanetary magnetic field (IMF) during the time of observations is predominately northward with the B_y component changing from positive to slightly negative. During this period Cluster is skimming the southern high latitude dusk magnetopause and reveals that reconnection is going on quasi-continuously with the reconnection site being most of the time tailward of the southern cusp and always near the satellite location (Retinò, et al., 2005). Detailed analysis of the three dimensional distribution function indicates that Cluster samples magnetosheath lines connected with geomagnetic field lines tailward of the cusps in both hemispheres (Bavassano Cattaneo et al., 2006). The evolution of the ionospheric convection measured by SuperDARN, together with IMAGE FUV observations of aurorae and DMSP particle precipitation data, confirms Cluster observations and shows that simultaneous reconnection poleward of both the northern and southern cusps occurs at a variable rate on the dusk part of the magnetosphere when the IMF clock angle is small.

Citation: Marcucci, M. F., I. Coco, D. Ambrosino, E. Amata, S. E. Milan, M. B. Bavassano Cattaneo, and A. Retinò (2008), Extended SuperDARN and IMAGE observations for northward IMF: Evidence for dual lobe reconnection, *J. Geophys. Res.*, *113*, A02204, doi:10.1029/2007JA012466.

1. Introduction

[2] It is thought that the greater part of the solar wind energy transfer to the magnetosphere-ionosphere system occurs through magnetic reconnection between the interplanetary magnetic field (IMF) and geomagnetic field lines. Since Dungey's work in the early sixties, it has been proposed that when the IMF is northward, it could reconnect with the lobe field lines at high latitudes, tailward of the magnetospheric cusps (the so-called "lobe reconnection") [*Dungey*, 1963]. Many in situ spacecraft observations confirm this hypothesis: *Gosling et al.* [1991, 1996]; *Onsager et al.* [2001]; *Fuselier et al.* [1995, 1997]; *Kessel et al.* [1996]; *Avanov et al.*, [2001]; *Safrankova et al.* [1998]; *Phan et al.* [2003]; *Retinò et al.* [2005] and, *Eriksson et al.* [2005]. Momentum transfer from the solar wind, once reconnection is occurring, results in large scale plasma convection in the polar ionosphere of both hemispheres. In the case of lobe reconnection, reconnected lines are first convected sunward due to the magnetic tension and then move anti-sunward along with the solar wind flow. Two reversed convection cells develop in the dayside polar ionosphere, with sunward flow in the center of the polar cap and anti-sunward flows at lower latitudes. Moreover, in case of lobe reconnection, the energy of the precipitating magnetosheath particles in the cusp is expected to decrease with decreasing magnetic latitude. These effects have been observed by means of ground based observations and low altitude orbiting satellites [*Cowley and Lockwood*, 1992, and references therein; *Ruohoniemi and Greenwald*, 2005, and references therein; *Chisham et al.*, 2004 and references therein]. If lobe reconnection occurs at one hemisphere only, reconnected lines are stirred inside the polar cap. If lobe reconnection occurs simultaneously at both hemispheres, tail magnetic flux is converted into new dayside closed flux [*Reiff and Burch*, 1985]. This can be an important mechanism by which the low latitude boundary layer is formed during northward IMF [*Song and Russell*, 1992], together with a cold and dense plasma sheet [e.g., *Øieroset et al.*, 2005, and references therein]. In situ evidence of dual lobe reconnection has been found in recent years through the analysis of proton and electron distribution functions [*Onsager et al.*, 2001; *Lavraud et al.*, 2006; *Bavassano Cattaneo et al.*, 2006]. Since the layer of doubly reconnected magnetosheath lines can be observed only when the spacecraft crosses it, it would be useful to identify the signatures of dual lobe reconnection in the polar ionosphere in order to understand to which extent dual lobe reconnection affects the magnetospheric dynamics on a large scale. To our knowledge the studies that did this are few. *Lockwood and Moen* [1999] based their

[1]Istituto di Fisica dello Spazio Interplanetario-INAF, Roma, Italy.
[2]Departement of Physics and Astronomy, University of Leicester, Leicester, UK.
[3]Swedish Institute of Space Physics, Uppsala, Sweden.

0148-0227/08/2007JA012466$09.00

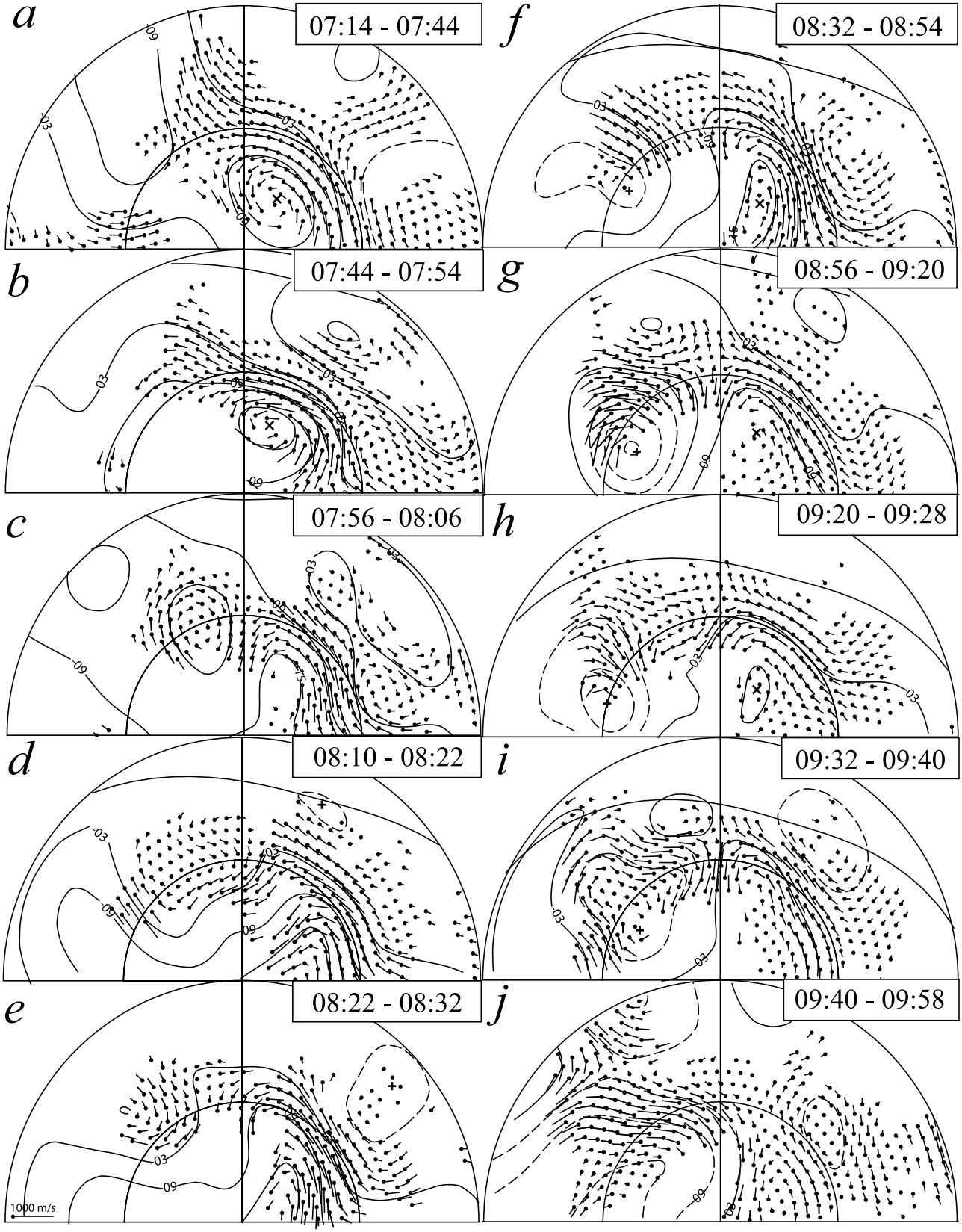

Figure 1. Convection maps of the SuperDARN measurements compiled for the time interval reported on the upper right corner of each panel. For each map 12 MLT is at the top, 18 MLT on the left and 6 MLT on the right. The magnetic latitude interval is 70°–90°.

explanation of the dynamics of auroral observations following an IMF reorientation as due to dual lobe reconnection, while *Imber et al.* [2006] showed, for the first time, the effect of dual lobe reconnection on ionospheric convection. In this paper, we will study the northern polar ionosphere during a period for which, based on a close examination of Cluster data near the southern magnetopause, *Bavassano Cattaneo et al.* [2006] suggested that dual lobe reconnection takes place. We present a detailed study of the Northern Hemisphere ionospheric convection and aurora as observed, respectively, by SuperDARN (Super Dual Auroral Radar Network) [*Greenwald et al.*, 1995] and by Imager for Magnetopause-to-Aurora Global Exploration (IMAGE) FUV [*Mende et al.*, 2000] for a large part of the period of Cluster observations. SuperDARN data are scarce in the Southern Hemisphere and will not be included in this study. First, the SuperDARN measurements are used to describe the overall dayside ionospheric convection, study its possible dependence on the IMF orientation and evidence signatures of lobe reconnection. Afterward, SuperDARN and FUV observations, with the DMSP (Defense Meteorological Satellite Program) auxiliary measurements [*Hardy et al.*, 1984], are used to confirm that dual lobe reconnection is occurring poleward of the northern and southern cusps at certain periods, transforming open lobe flux into dayside closed flux.

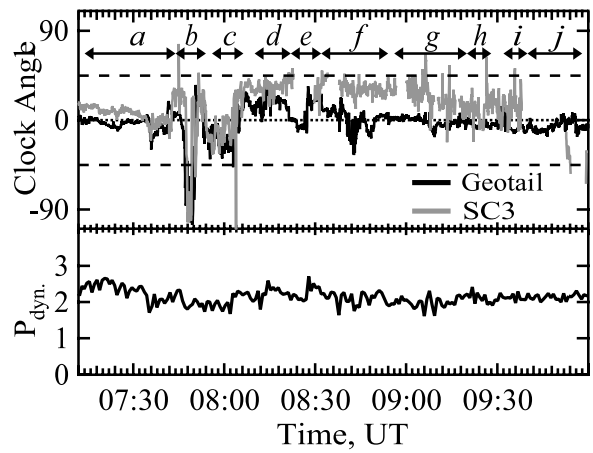

Figure 2. Top panel: magnetic field clock angle measured by SC3 in the dusk high latitude southern magnetosheath (grey line); IMF clock angle measured by Geotail in the solar wind near the dawn flank of the magnetopause (black line). The GSM coordinates system is used. SC3 data are not plotted when the satellite is in the magnetosphere or in the magnetosheath boundary layer. SuperDARN convection during this period is summarized by the labeled arrowed lines (see text for details). Bottom panel: solar wind dynamic pressure measured by Geotail. Geotail data are shifted in time by 2 min to match SC3 data.

2. Observations

2.1. Summary of Cluster Observations Tailward of the Southern CUSP

[3] On 3 December 2001, between 07:20 and 12:00 UT, Cluster was skimming the high-latitude duskside magnetopause tailward of the Southern Hemisphere cusp. During this period the IMF was predominantly northward, apart from very short periods, with the B_y component being mainly positive in the first part of the event and negative afterward, and with a positive B_x component. *Retinò et al.* [2005] analyzed data from the Cluster Ion Spectrometry (CIS) and the Flux-Gate Magnetometer (FGM) experiments on board Cluster spacecraft SC1, SC3 and SC4 and showed fluid and kinetic evidence of magnetic reconnection going on continuously for about four hours whenever the IMF was northward. Their observations are consistent with magnetic reconnection occurring tailward of the cusp, indicate that Cluster is close to the reconnection site and give evidence for component merging. Moreover *Retinò et al.* [2006] further studied this period and described the micro-scale structure of the separatrix region in the proximity of the reconnection site. Finally, *Bavassano Cattaneo et al.* [2006] performed a detailed analysis of the three-dimensional distribution functions measured by SC3 and suggested that reconnection is occurring simultaneously tailward of the southern cusp and at a reconnection site in the Northern Hemisphere. In fact, during particular time intervals when SC3 is in the magnetosheath boundary layer, three populations can be identified in the measured distribution functions: the incident magnetosheath population, the population reflected at the southern (nearest) reconnection site located tailward of the cusp, and the population reflected at a reconnection site in the Northern Hemisphere. The population reflected at the reconnection site closer to Cluster moves toward the Northern Hemisphere (upward and sunward) parallel to the magnetosheath magnetic field, while the population reflected at the northern reconnection site reaches Cluster along the magnetosheath magnetic field in the anti-parallel direction. It is difficult to ascertain the exact position of the northern reconnection site, but given the northward orientation of the IMF, *Bavassano Cattaneo et al.* [2006] speculate that it can be located tailward of the northern cusp. A clear event of this type is observed in the 09:39:48–09:40:12 UT interval when Cluster SC3 is in a magnetosheath boundary layer on closed magnetic fields lines that appear to map tailward of the southern cusp and, presumably, also of the northern cusp.

2.2. The Northern Dayside Ionospheric Convection Pattern During the Event

[4] We use line-of-sight Doppler velocities, measured by eight SuperDARN radars, to produce global convection maps of the northern ionosphere according to the technique of *Ruohoniemi and Baker* [1998]. Since in the present case the data coverage is excellent, the empirical model which is built into such technique has little effect on the final solution. Each convection map, computed every two minutes in the interval 07:20–12:00 UT, has been visually inspected. After 10:00 UT very large flow vortices affect the dayside convection. Such vortices are probably associated with solar wind pressure variations (not shown) and are not purely related to magnetopause reconnection; therefore, from now on, we will concentrate on the 07:20–10:00 UT period. The visual inspection of the convection maps reveals that characteristic patterns are observed for extended time intervals during the period under study. For each such interval average convection maps have been computed. In

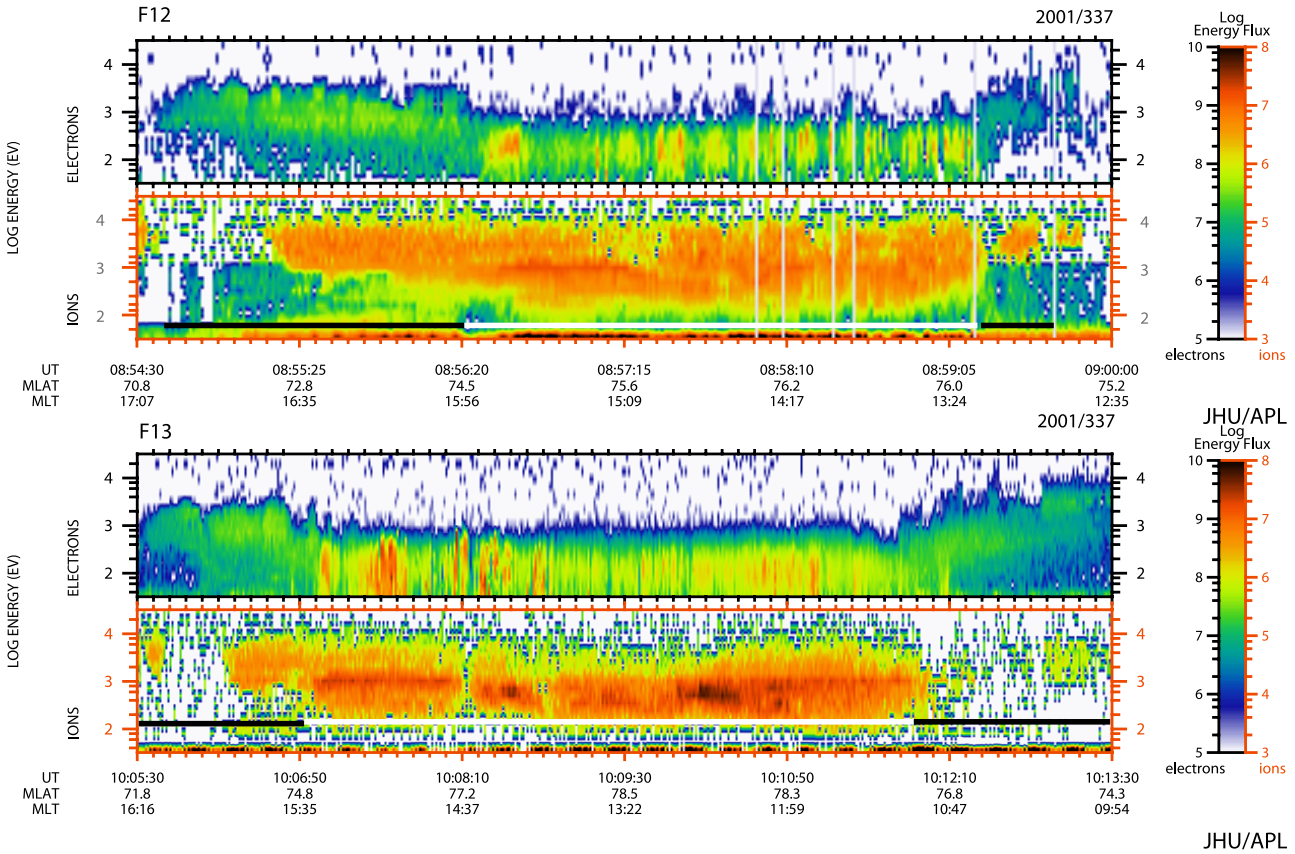

Figure 3. Electron and ion energy spectrograms measured by the DMSP satellites F12 and F13, respectively. The black bold lines indicate the regions of high energy magnetospheric electron precipitation, while the white lines indicate the LLBL-Cusp like precipitation regions.

Figure 1 the dayside sectors of ten average convection maps are shown with the relative time periods. When the convection pattern is not stable for more than four minutes the average map is not computed and not shown in the figure. These maps describe the dayside ionospheric convection throughout the event. In interval a) a clockwise polar cap cell is observed at dawn, with a post noon antisunward flow at lower latitudes. During b) the clockwise dawn polar cap cell is still present but the duskside lower latitude flow now is due westward. During c) a counter-clockwise cell appears in the post noon sector together with the clockwise dawn cell. In d) the most prominent feature is the clockwise dawn polar cap cell which expands to the post noon polar cap sector; the flow around noon is directed westward and the dusk counter-clockwise cell has weakened. In e) the clockwise cell seems to be confined to the pre-noon sector, even if it must be noted that the data coverage above 80° Magnetic Latitude (MLAT) in the post noon sector is reduced; however, flows around noon are now directed in the sunward direction and the counter-clockwise cell in the post noon sector is strengthening. In f) the eastward and sunward directed flow of the postnoon counter-clockwise cell strengthens; in g) two symmetric reverse convection cells are observed; in h) the duskward counter-clockwise cell is reduced; in i) and j) the duskward counter-clockwise cell becomes dominant.

[5] Figure 2 compares the ionospheric convection patterns described in Figure 1 with the solar wind and magnetosheath conditions. The upper panel displays: 1) double-arrowed segments which depict the time intervals pertaining to each of the Figure 1 panels and are labeled accordingly, 2) the IMF clock angle ($\tan^{-1}(B_y/B_z)$) measured by Geotail, which is in the solar wind at the dawn flank of the magnetopause, 3) the clock angle measured by Cluster SC3 at the dusk high latitude southern magnetosheath, roughly at the same X position of Geotail (data are not plotted when SC3 is in the magnetosphere). The lower panel shows the solar wind dynamic pressure measured by Geotail. All Geotail data have been forward shifted in time by 2 minutes, so that the main variations of the Geotail and SC3 clock angles coincide in time. This appears to be reasonable because the IMF variations are expected to reach first Geotail in the solar wind than SC3 in the magnetosheath. On the other hand no time shift has been applied to the segments referring to ionospheric convection. Starting from the lower panel, we notice that the solar wind dynamic pressure does not shown any relevant variation. Moving to the upper panel, we observe that the Geotail and SC3 clock angles show similar behaviors, even if some large differences between the two are observed for short intervals and the clock angle is generally larger at SC3. As already stated, the IMF during the time of observation is predominately northward with the B_y component being mainly positive in the first part of the interval and slightly negative afterward, apart from a very short period at about 07:46 UT. The B_x component (not shown) is positive both at SC3 and Geotail.

Before comparing the variations of clock angles and ionospheric patterns, we remark that both SC3 and Geotail observed a positive and larger clock angle for at least one hour before the period shown in the figure.

[6] During a), when the ionospheric convection is characterized by a clockwise dawn cell, the clock angle measured by SC3 is positive; the IMF clock angle measured by Geotail is only slightly positive. The westward flows observed around noon during b) and, at higher latitudes, during d) occur during periods when the clock angle is around 40° (enhanced B_y positive component), as measured by SC3. The c) and e) patterns, when a counter-clockwise cell as observed in the dusk sector seems to start, are associated with short IMF rotations, with only the first one observed by SC3, from B_y positive to B_y slightly negative. After 08:35 (periods f) g) h) i) and j)) the convection slowly becomes dominated by the duskside counter-clockwise convection cell. This occurs while the IMF clock angle measured at Geotail reduces to zero and then becomes slightly negative; the SC3 clock angle also decreases towards zero, but at a somewhat later time than Geotail.

2.3. The Open-Closed Boundary Variability and Relative Ionospheric Flows

[7] We showed in section 2.1 that, in the 09:39:48–09:40:12 UT interval, Cluster SC3 is in a magnetosheath boundary layer on closed magnetic fields lines which probably map tailward of both the southern and the northern cusps [*Bavassano Cattaneo et al.*, 2006]. However, the layer of doubly reconnected magnetosheath lines can be observed only for a short time when the spacecraft crosses it. To determine whether dual lobe reconnection proceeds sufficiently long and is efficient enough to affect the large-scale magnetospheric dynamics, we have to study how the area of the open polar cap changes. In fact, when reconnection is occurring simultaneously tailward of both cusps we expect that the area of the open polar cap will be decreasing. This could be evidenced through displacements of the open-closed field line boundary (OCB) projection in the ionosphere. In the case under study, we expect that dual lobe reconnection will lead to a poleward motion of the OCB in the dayside. As Cluster is on the dusk side of the magnetosphere at about 19 Magnetic Local Time (MLT) and as the IMF B_y is much less than IMF B_z we expect that the footprints of the re-closing magnetic field lines, sampled by Cluster, are located approximately in the post-noon sector. Moreover, the convection patterns show that intense sunward and eastward flows develop around 15 MLT after 08:35 UT, when the duskside counter-clockwise cell develops. Hence we concentrate in the postnoon sector and try to identify the latitudinal displacements of the OCB position along the 15 MLT meridian. As described by *Milan et al.* [2003] the poleward edge of high energy (1–10 keV) electron precipitation is considered to be a proxy of the OCB. Satellite particle measurements along low altitude orbits can be used to readily identify this precipitation boundary, but only at a particular point and time, when the satellite enters or exits the polar cap. On the other hand, the OCB can also be identified from the auroral luminosity pattern and from the HF radar backscatter; by these means the OCB position can be monitored continuously over a wide range of MLT [*Milan et al.*, 2003; *Chisham et al.*, 2004 and references therein]. Here we use a combination of IMAGE S13 auroral images, SuperDARN data and DMSP low altitude particle measurements to identify the OCB in the postnoon sector throughout the interval under study. Figure 3 shows electron and ion energy-spectrograms measured by the DMSP satellites F12 and F13 from 08:54:30 to 09:00:00 UT and from 10:05:30 to 10:13:30 UT, respectively. The horizontal black lines above the time axes indicate the precipitation of high energy magnetospheric electrons, while the white lines indicate LLBL/Cusp-like precipitation. In Figure 4 observations of the northern high latitude region made by the S13 sensor on board IMAGE

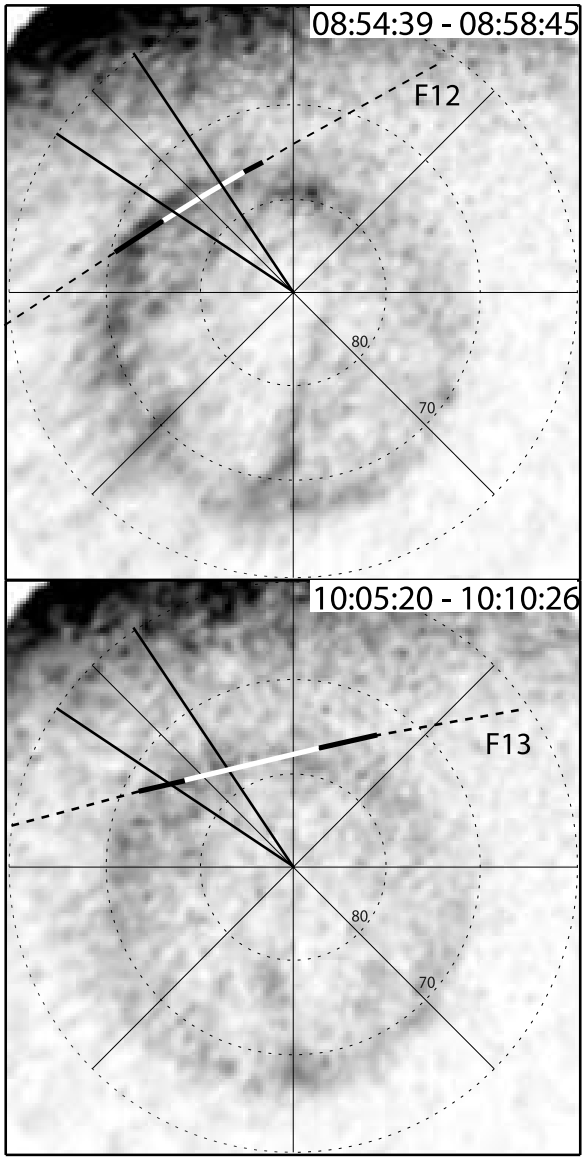

Figure 4. Observations of the high latitude Northern Hemisphere made by the S13 sensor on board IMAGE for the two time intervals reported on the upper right corner of each panel. The corresponding passes of the DMSP satellites F12 and F13 are also overplotted. The black dashed line is the orbit track, the bold dark lines correspond to high energy electron precipitations, while the bold white lines correspond to LLBL/Cusp type precipitation.

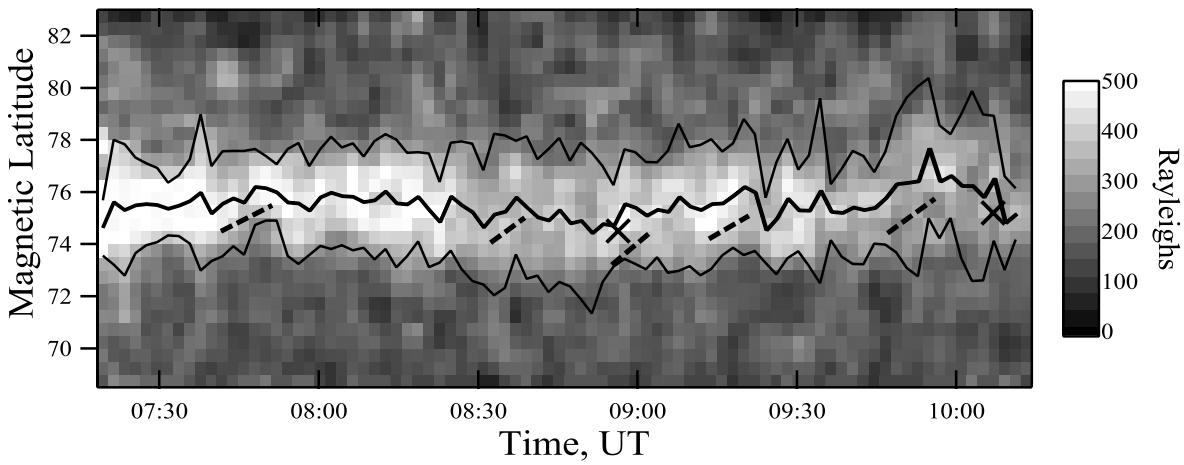

Figure 5. Keogram of the S13 measurements between 68° and 83° MLAT for the 07:18–10:14 UT interval, built through the temporal sequence of the S13 intensity averaged, for each image, in intervals of 0.5° MLAT between 14:15 and 15:45 MLT. The black crosses at 08:56 UT and 10:07 UT mark the MLAT where the F12 and F13, at 15:56 MLT and 15:39 MLT respectively, observe the drop in the high energy electron precipitation. The bold and the two light lines represent the latitude of the peak and the width of the Lorentzian fit of the auroral oval computed for the vertical profile of each time of observation.

are shown for two time intervals during the event: 08:54:39–08:58:45 UT and 10:05:20–10:10:26 UT in the upper and lower panel respectively. Both S13 images are overplotted with dashed lines corresponding to the F12 and F13 DMSP passes shown in Figure 3 and with black and white lines corresponding to those of Figure 3. The auroral oval is clearly visible in these images, more intense in the upper than in the lower one. A transpolar arc is also present and its orientation clearly changes from dawnward to duskward passing from the upper to the lower image. The dynamics of this arc and its relationships with the ionospheric plasma convection will be discussed in detail in a subsequent paper. Concentrating on the dayside dusk sector, the observed luminosity is very intense below 60° MLAT due to the airglow, but decreases moving to higher MLAT, to the extent that the auroral oval is clearly distinguishable at about 75° MLAT. Crossing the maximum luminosity of the auroral oval and moving towards the pole, enhanced emissions continue to be observed and sometimes appear as a secondary intensity peak, as in the upper image. In the upper panel, we notice that the high energy magnetospheric electrons precipitation (black line segment between 16 and 17 MLT) is observed by F12 in correspondence with the maximum of the auroral oval intensity. Then the transition to LLBL-Cusp like precipitation is observed by F12 at about 08:56:20 UT roughly matching the central time of the S13 image. A similar transition is observed by F13 at 10:06:50 UT (this time close to 15 MLT) during the time interval pertaining to the S13 lower image. In conclusion, the comparison of DMSP and IMAGE observations suggests that, especially for the sector around 15 MLT, the maximum of the auroral oval luminosity coincides with the poleward edge of the high energy electron precipitation and therefore with the OCB position.

[8] We have studied the temporal evolution of the OCB latitudinal position close to the 15 MLT meridian. For that purpose, Figure 5 displays, on a gray scale, the 15 MLT S13 keogram between 68° and 83° MLAT for the time interval 07:18–10:14 UT. The keogram has been generated by computing, for each FUV image (i.e., approximately every 2 min), the average of the S13 intensity between 14:15 and 15:45 MLT (Magnetic Local Time) in intervals of 0.5° MLAT; the data have been smoothed with a Gaussian filter to reduce the noise. The keogram suggests that the OCB be located at approximately 75°–76° MLAT, but several displacements from this average position seem to occur. To better quantify them, we perform a fit of the magnetic latitude profile of the keogram for each time of observation. The function used to do the fit is the sum of a Gaussian and a constant, to represent the airglow and the background, a Lorentzian, to represent the auroral oval and another Gaussian to represent the secondary emissions poleward of the auroral oval. The only constraint used while doing the fit is that the background constant must be positive. The ratio of the sum of the square of the deviations (i.e., the difference between the fitted and the actual data) to the sum of the square of the data, is less than 0.01 for all the profiles. In Figure 6 two profiles, solid lines, with the relative fit, dashed lines, are shown. We wish to remark that the 09:57:07 UT profile (lower panel) represents one of the worst cases as it is one of the few for which the above mentioned ratio approaches 0.01; nevertheless, the auroral oval profile is still well represented by the Lorentzian, whose maximum intensity latitude and width are identified by the vertical dashed lines and double arrowed horizontal lines, respectively. For each profile the latitude of the peak of the Lorentzian and its width are overplotted on the keogram of Figure 5 as a bold and two light lines. The black crosses at 08:56 UT and 10:07 UT mark the MLAT where the drop of the high energy electron precipitation is observed by the F12 satellite at 15:56 MLT and by the F13 satellite at 15:39 MLT, respectively. We notice that both crosses fall very close to the enhanced keogram luminosity and to the MLAT corresponding to the Lorentzian peak. On

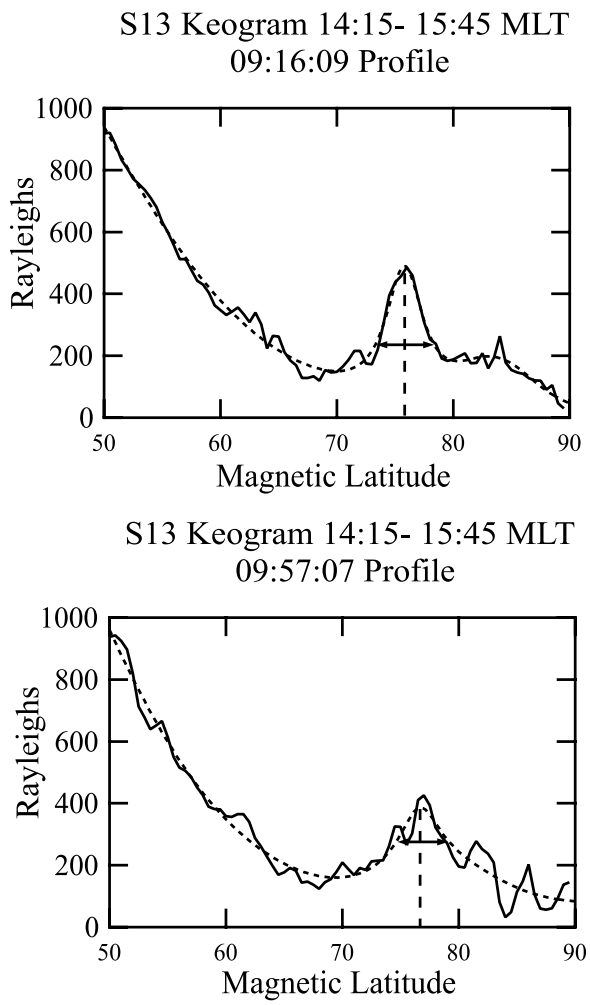

Figure 6. S13 intensity averaged between 14:15 and 15:45 MLT in 20 intervals of 0.5° MLAT, from 50° to 90° MLAT, at 09:16:09 UT and 09:57:07 UT (solid lines). The relative fits (see text for details) are drawn as dashed lines. The vertical dashed lines and double arrowed horizontal lines represent, respectively, the maximum intensity latitude and the width of the Lorentzian which is meant to reproduce the auroral oval latitude profile.

these grounds, we make use of the luminosity peak MLAT to monitor the position of the OCB. In the period 07:20–10:10 UT we have identified 5 main poleward movements of the OCB and have highlighted them by dashed segments below the peak bold line.

[9] The SuperDARN spectral width measurements can be used to infer the position of the OCB (see the Discussion section for details). In our case, the study of the OCB position around 15 MLT can be performed using Hankasalmi radar data (and in particular beam 12, which is directed almost meridionally and crosses the OCB, as

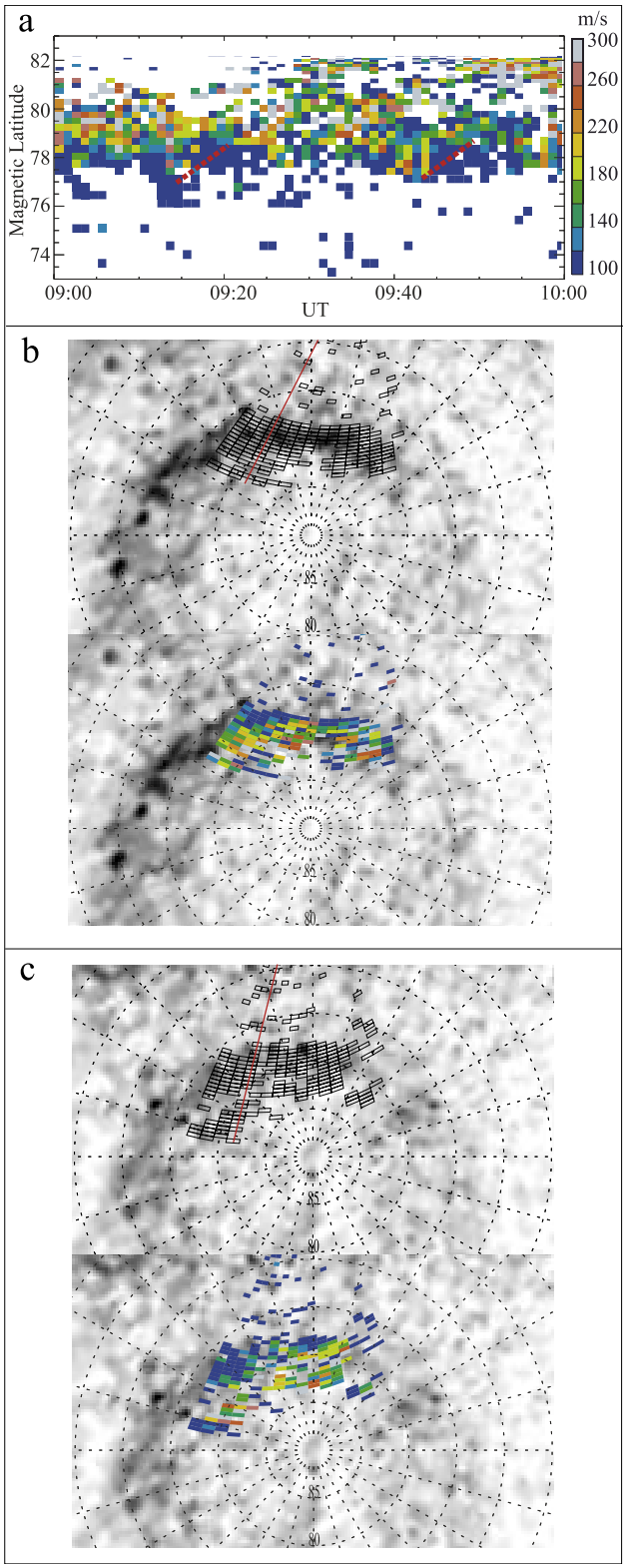

Figure 7. Panel (a): Hankasalmi beam 12 spectral width as a function of time and magnetic latitude in the 09:00–10:00 UT interval. Panel (b) and (c): S13 images for the 08:56:42–08:58:43 and 09:47:45–09:49:57 UT intervals. In the upper parts of panels (b) and (c) the Hankasalmi data coverage and the line of sight of beam 12 (red line) at 08:56–08:58 and 09:48–09:50 UT are overplotted on S13 images; in the lower parts of panels b) and c) the Hankasalmi spectral width data are overplotted on the S13 images.

defined by the auroral luminosity, very close to 15 MLT). This can be done after 09:00 UT when the radar beams span the afternoon sector, while for the earlier part of the event, the Hankasalmi radar beams cross the OCB mostly in the pre-noon sector. Figure 7 shows this study for the last two poleward movements of the OCB. Panel a) presents a plot of the Hankasalmi beam 12 spectral width as a function of time and magnetic latitude between 09:00 and 10:00 UT. Panels b) and c) display the S13 average images for the 08:56:42–08:58:43 UT and 09:47:56–09:49:57 UT intervals, respectively. In the upper parts of these panels the corresponding Hankasalmi data coverage and the position of beam 12 (red line) are overplotted on the S13 images; in their lower parts the Hankasalmi spectral width is overplotted on the S13 images. The spectral width appears to have high values (above 150 m/s) at higher MLAT and lower values (below 150 m/s) at lower MLAT. The average boundary between the two regions falls between 77° and 78° MLAT. However, it is evident that around 09:20 and 09:50 UT this boundary moves to higher latitudes (above 78°), as highlighted by the dashed red lines. This is in agreement with the latitudinal displacements of the OCB observed in the S13 keogram in the same interval. Looking at panels b) and c), we note that low spectral widths correspond to the maximum of the auroral oval luminosity, which we have shown to coincide with the poleward edge of the high energy electron precipitation, and therefore with the OCB position for 15 MLT. Poleward of the OCB the spectral width is higher. Moreover, a very high spectral width band is observable in the plot of the spectral width above 80° after 09:20 UT, often separated from the lower latitude backscatter signals by a gap in the echoes; this band appears to coincide with the luminosity peak which is sometimes observed poleward of the auroral oval in the S13 data (panel c).

[10] We shall now compare the OCB poleward movements as seen by IMAGE with the ionospheric convection as reconstructed through SuperDARN data. The first poleward displacement, at 07:44 UT, corresponds to the changing of the flow, in the postnoon sector, from being anti-sunward to being strongly westward, as the convection changes from type a) to type b), in association with the IMF clock angle enhancement of 07:44 UT (see Figure 1). We will not discuss this latitudinal displacement further. Figure 8 displays, on the left, 2-min SuperDARN convection maps at the time of the other four poleward movements of the auroral oval. For comparison, 2-min convection maps taken a few minutes before each movement are shown on the right of the figure. It can be noted that the poleward displacements of the OCB occur during periods when the sunward flows at 15 MLT are enhanced and perpendicular to the OCB itself (identified with the auroral oval) and seem to cross it. Conversely, during the nearby periods, when the position of the OCB is stable or moving to lower latitude (as evidenced by the keogram), the flow velocity across the OCB is small or zero. This is clearly seen in the 09:10 and 09:32 UT convection maps, when the dusk counter-clockwise cell is completely contained in the auroral oval. The S13 keograms generated for the sector around 12 MLT and 9 MLT (not shown) do not present any of the signatures observed in the 15 MLT keogram. On the other hand, the dawnside clockwise cell appears to be always confined in the polar cap.

3. Discussion

[11] Visual inspection of the Northern Hemisphere SuperDARN convection maps presented in this study has shown that sunward flows are continuously observed in the noon sector of the polar cap under northward IMF conditions. These flows are eastward or westward directed according to whether the sign of B_y was slightly positive or negative. In fact, the convection seems to be dominated by a dawnside (duskside) clockwise (counter-clockwise) polar cap cell during periods of mostly positive (negative) clock angle and two symmetric reversed cells develop in the polar cap when the clock angle approaches zero. These features can be explained in terms of reconnection between the IMF and the magnetospheric field lines tailward of the northern cusp [*Dungey*, 1963; *Crooker*, 1979; *Reiff and Burch*, 1985; *Ruohoniemi and Greenwald*, 2005].

[12] In our observations the response of the dayside ionospheric flows following an IMF rotation is of the order of a few minutes; for instance, at 07:42 UT when the clock angle approaches 45°, the flows at noon become more westward in about 2 minutes. However, if the IMF rotation causes a global change of the ionospheric convection, for example from a dawn clockwise cell to a dusk anti-clockwise cell, it takes more than ten minutes for the reconfiguration to occur. In fact, for the short-lived rotations of 07:54 UT and 08:20 UT, the expected convection pattern for the new IMF orientation never became established.

[13] We note that in this case northern lobe reconnection is going on throughout the time of observation despite the fact that the dipole tilt is unfavorable and B_x is positive [*Crooker and Rich*, 1993; *Lockwood and Moen*, 1999]. In fact, Cluster observations indicated that southern lobe reconnection is continuous.

[14] Using DMSP data and IMAGE S13 observations we have found that, during the interval 08–10 UT, four poleward movements of the OCB near the 15 MLT meridian were observed in the Northern Hemisphere. This signature can be due to dual lobe reconnection occurring tailward of the northern and southern cusps. During each of the four poleward movements the sunward/westward ionospheric flows, which are part of the duskside counter-clockwise convection cell in the polar cap, are enhanced and seem to cross the OCB. In nearby times these flows are reduced or appear to be tangent to the OCB, so that the duskward cell is completely contained in the polar cap. *Imber et al.* [2006] showed that enhanced sunward flows through the OCB can be explained in terms of dual lobe reconnection. They support this interpretation through the observation that intense sunward flows, occurring at two northward turnings of the IMF, are accompanied by enhancements of auroral luminosity that can be associated with an increase in magnetosheath particle precipitation due to two reconnection sites simultaneously active tailward of both the northern and the southern cusp. Moreover, *Imber et al.* [2006] also speculate that, for dual lobe reconnection to occur, the IMF clock angle should be less than 10°.

[15] We also interpret our observations as the results of lobe flux re-closure. In our case the sunward flows crossing

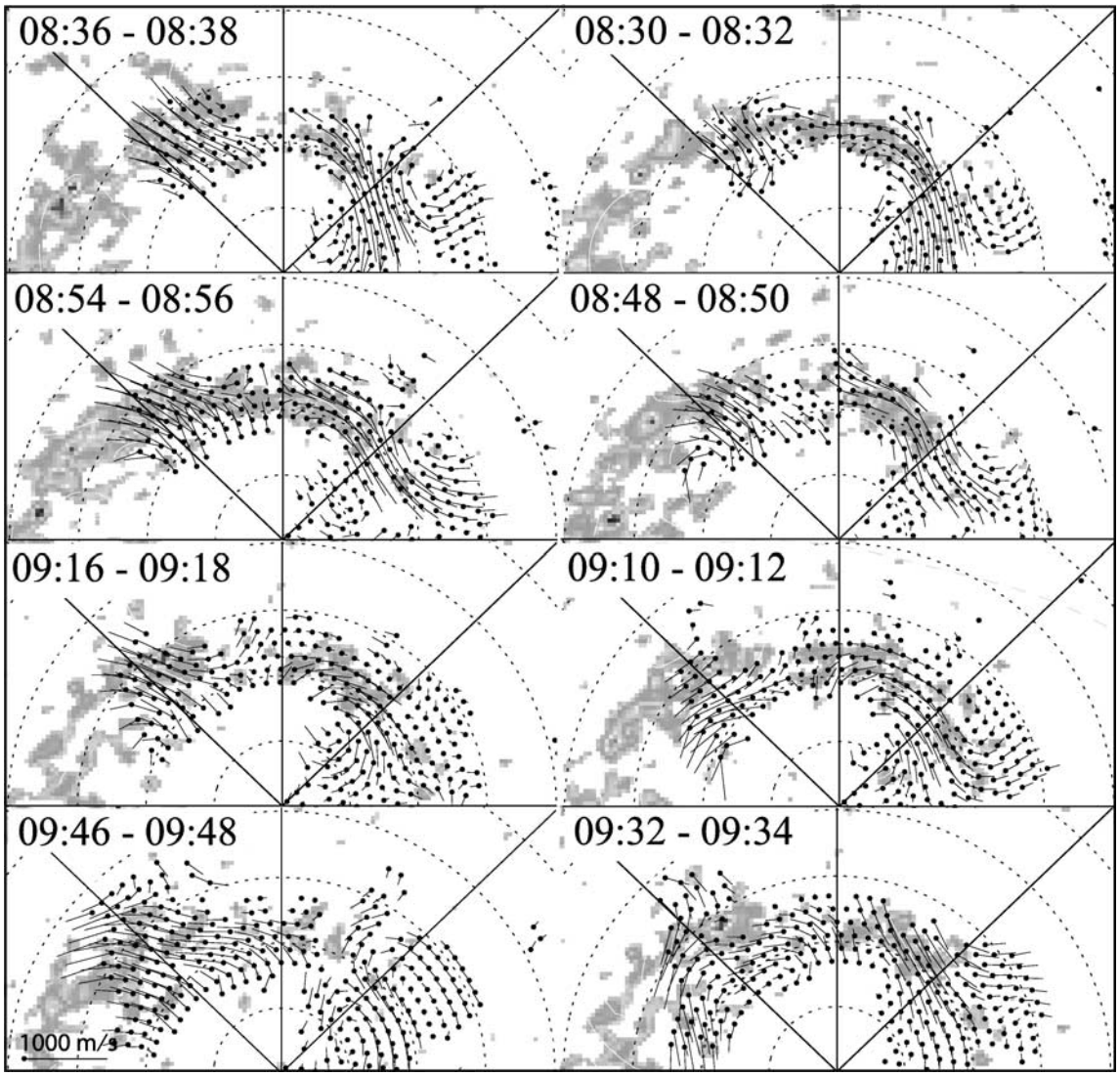

Figure 8. SuperDARN convection maps computed for 2 min scans at the time intervals reported on the left upper corner of each map. The corresponding S13 images are overplotted on the maps. 12 MLT is at the top, 18 MLT on the left and 6 MLT on the right. The magnetic latitude interval is 70°–90°. On the left are reported observations during the poleward movements of the auroral oval, on the right observations taken for nearby time intervals.

the OCB are accompanied by poleward movements of the OCB itself. In our event the Geotail clock angle is close to zero in the interval 08–10 UT, while the SC3 clock angle is ~10° between 09 and 10 UT. In fact, signatures for dual lobe reconnection become evident between 08 and 10 UT. We note that the variability of the OCB position, with the corresponding ionospheric flow modulation, indicate that dual lobe reconnection occurs sporadically and/or at a variable rate. Moreover, we note that dual lobe reconnection seems to occur only on the dusk side of the magnetosphere, notwithstanding the IMF clock angle being small. The burst of dual lobe reconnection associated with the poleward movement at 09:40 UT confirms Cluster in situ observations of simultaneous reconnection tailward of both the northern and the southern cusp [*Bavassano Cattaneo et al.*, 2006].

[16] During southward IMF, the boundary between low and high Doppler spectral width echoes or the equatorward edge of the observed backscatter can be used as a proxy of the polar cap boundary [see *Milan et al.*, 2003 and references therein]. The situation is different for northward IMF. *Milan et al.* [2003] found that, during northward IMF periods, significant but low level auroral luminosity appears to be co-located with magnetosheath ion reversed dayside precipitation, so that they assume that the OCB coincides with the equatorward edge of this luminosity (see second panel of their Figure 5). In these cases the radar backscatter is uncorrelated with the OCB. On the other hand, there are cases, during northward IMF, in which the poleward edge of the backscatter region may be associated with the ionospheric footprint of the reconnection line located at the high

latitude magnetopause tailward of the cusp [*Chisham et al.*, 2004]. S13 observations for the event under study seem to show two distinct luminosity regions in the dayside dusk sector. The lower latitude one appears to be associated with the boundary of the high energy electron precipitation in the DMSP data and with the boundary, at low latitudes, between low and high spectral width echoes for beam 12 of the Hankasalmi radar. The polar cap luminosity enhancement, instead, seems to be associated, for the last part of the interval, with the high latitude band of high spectral width seen by Hankasalmi beam 12 (see panel a) of Figure 7). We speculate that, for this event, we may identify the OCB as the peak of the auroral luminosity or the high-low spectral width boundary, and the footprint of the lobe reconnection line as the high latitude distinct enhancement of luminosity co-located with the high spectral width band. In fact, the comparison of SuperDARN convection maps and S13 observations shows that for the period 08–10 UT the high latitude luminosity coincides with the poleward boundary of SuperDARN measurements in the 12–15 MLT sector (Figure 8).

[17] We note that if a part of magnetosheath flux is reconnecting simultaneously tailward of both the northern and southern cusp, the projection of the merging line in the northern and southern ionosphere, respectively, should coincide with the OCB. The OCB and the merging line appear to be separated when lobe reconnection is active at one hemisphere only or when it proceeds at a different rate in the two hemispheres [*Lockwood and Moen*, 1999]. In particular, if the reconnection rate is faster in the Northern Hemisphere, magnetosheath lines reconnected with the northern lobe lines will over-drape around the dayside magnetopause and the merging line projection in the Northern Hemisphere will be distinct from the OCB and poleward of it. In the case under study the favored hemisphere for lobe reconnection to occur would be the Southern one, since we are at the December solstice and the B_x component is positive. In fact, Cluster measurements provide evidence for continuous reconnection at the dusk southern magnetopause tailward of the cusp. Therefore we should observe the over-draping effect in the Southern Hemisphere, not in the Northern one. Moreover, since both the IMF clock angle measured by Geotail and the clock angle measured by SC3 are less than 10°, we would expect dual lobe reconnection to occur continuously in the interval 09–10 UT. Contrary to this expectation, our observations in the Northern Hemisphere seem to show that: the OCB and the merging line appear to be separated and dual lobe reconnection occurs sporadically. We speculate that the strong inclination of the dipole in the ZY plane during this period could play an important role in decoupling northern and southern lobe reconnection. In this respect, we note that dual lobe reconnection seems to occur only on the dusk side of the magnetosphere despite the fact that the IMF clock angle is small.

[18] In Figure 9 a sketch of the dayside dusk sector, relative to a situation when one of the poleward OCB movements is just ended, is proposed. In this figure, L is the portion of the OCB along which magnetic field lines are transformed from open to closed, L_{rec}, the dashed line, is the projection in the ionosphere of the dusk part of the northern lobe merging line, $\Delta\lambda$, the dot-dashed line, is the latitudinal displacement of the OCB along the 15 MLT meridian for a poleward movement of duration $\Delta\tau$. SuperDARN flow vectors for the time interval 09:16–09:18 UT are overplotted on the picture.

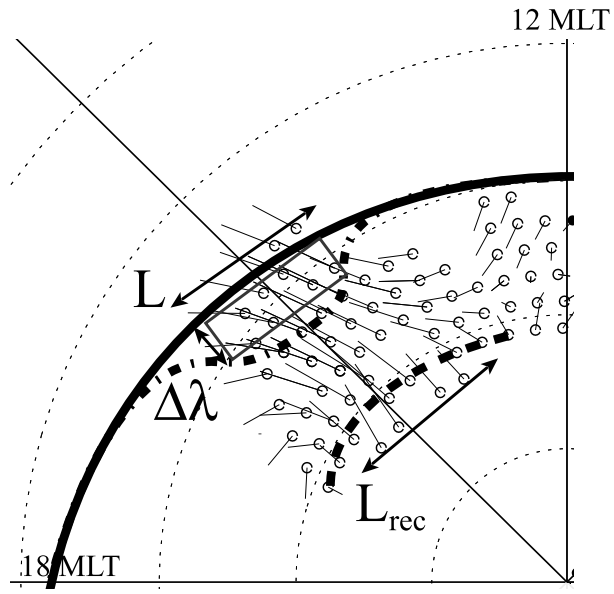

Figure 9. Sketch of the OCB before the occurrence of dual lobe reconnection (heavy line), of the new position of the OCB when dual reconnection has been going on for a time interval $\Delta\tau$ (dotted-dashed line) and of the projection of the northern lobe reconnection line for the case under study (dashed line). The SuperDARN flow vectors for the 09:16–09:18 UT interval are overplotted on the drawing.

[19] In case of dayside low latitude reconnection during southward IMF, the initial equatorward displacement of the OCB is localized and determined by the burst of reconnection; afterward, the response of the magnetosphere-ionosphere system, which has to adapt to a new equilibrium state, reduces the initial local displacement in favor of an expansion of the whole polar cap [*Cowley and Lockwood*, 1992; *Lockwood and Morley*, 2004]; besides, the ionospheric anti-sunward flows crossing the OCB are the effect of such a response and are expected to be observed with a certain delay with respect to the equatorward OCB migration. Bearing in mind that the observations under study pertain to a northward IMF case of dual lobe reconnection, we note that, in Figure 5, the OCB actually seems to slightly relax back after each poleward movement. Moreover, the enhanced sunward flows crossing the OCB in correspondence with the OCB poleward movements seem to be somewhat delayed with respect to such movements (not shown). Lets consider the $\Delta\lambda$ displacements as the effect of the burst of dual lobe reconnection only. This could be a simplification, since the characteristic time response of the magnetosphere-ionosphere system to a variation in the dayside reconnection is about 10 min [*Lockwood et al.*, 2006] which is comparable with the duration of the poleward movements, although we are considering the dual lobe reconnection case. The magnetic flux re-closed by dual lobe reconnection going on for an interval of time $\Delta\tau$ can be approximated as $L\Delta\lambda B$. On the other hand, if we assume that all the flux reconnecting in the Northern Hemisphere at

dusk is reconnecting also in the Southern Hemisphere, the open magnetic flux transformed to closed magnetic flux can also be expressed as $V\Delta\tau L_{rec}\ B$, where V is the average ionospheric velocity normal to L_{rec}. From SuperDARN and S13 observations it can be seen that: 1) the assumption of total re-closing of northern and southern reconnected lobe flux could be valid since almost all the sunward flows departing from the projection of the merging line in the polar cap cross the auroral oval (see Figure 8 right column panel b, c, d); 2) the average velocity normal to the merging line is about 500 m/s; 3) $L_{rec} \sim L$. We put the time interval $\Delta\tau \sim 8$ min, approximately the duration of the poleward displacements of the OCB boundary as evidenced in the S13 keogram. In conclusion, the expected latitudinal displacement due to dual lobe reconnection is approximately $V\Delta\tau \sim 220$ km, corresponding to $\sim 2°$. Even if this is only a very rough estimate, it appears to be consistent with the observed latitudinal displacement.

[20] If the footprint of the lobe reconnection line were identified as the high latitude enhancement of luminosity co-located with the high spectral width band, it would coincide with the poleward boundary of SuperDARN measurements in the 12–15 MLT sector in the convection maps of Figure 8. We note that the position of this boundary seems to be the same at the times of the poleward displacements of the OCB (right column of Figure 8) and at nearby times (left column of Figure 8). Therefore during the poleward movement of the OCB there is a narrowing of the latitudinal interval between the OCB and the northern lobe reconnection line projection at dusk, indicating a possible reduction of the over draping as expected once that dual lobe reconnection starts. Furthermore, this is more consistent with the re-closure of open flux in the dayside by lobe reconnection than with a poleward movement of the OCB caused by a contraction of the polar cap due to closure of open flux in the tail [*Lockwood and Moen*, 1999].

4. Summary

[21] We presented a detailed study of SuperDARN data and IMAGE FUV observations of aurorae in the Northern Hemisphere for a period when the IMF is predominately northward with the B_y component changing from positive to slightly negative. Cluster plasma and magnetic field observations, during the same period, show that lobe reconnection is continuously going on in the Southern Hemisphere at dusk. Moreover, Cluster observations show evidence that dual lobe reconnection is occurring at particular time intervals. The visual inspection of SuperDARN convection maps throughout the period of study shows that the northern high latitude ionospheric convection is determined by the orientation of the IMF and that lobe reconnection is occurring at the Northern Hemisphere despite the fact that the dipole tilt is unfavorable and B_x is positive [*Crooker and Rich*, 1993; *Lockwood and Moen*, 1999]. DMSP, IMAGE S13 and SuperDARN observations show that, during the 08–10 UT interval, four poleward movements of the OCB are associated with enhanced sunward/westward velocity flows crossing the OCB itself. We interpret this as the result of lobe flux re-closure occurring sporadically in the dusk sector, with the poleward movement of 09:40 UT confirming Cluster in situ observations of dual lobe reconnection.

[22] Finally, we would like to point out that this work and those by *Retinò et al.* [2005, 2006] and *Bavassano Cattaneo et al.* [2006], provide a comprehensive study of the effects of reconnection from the microscale of the separatrix region to the global scale of the magnetosphere.

[23] **Acknowledgments.** This work was supported by the Italian National Program for Antarctic Research, PNRA, and by the Agenzia Spaziale Italiana (ASI contract I/035/05/0). M.F. Marcucci thanks G. Consolini for his useful suggestions. We would like to thank S. B. Mende and the FUV team at UC Berkeley for the IMAGE FUV data and for the FUVIEW software used to construct the keogram. We thank S. Kokubun and L. Frank for Geotail magnetic field and plasma data, respectively, downloaded from CDAWeb. The DMSP particle detectors were designed by Dave Hardy of AFRL, and data have been obtained from JHU/APL. We thank D. Hardy, F. Rich, and P. Newell for its use. We thank all of the principal investigators of the SuperDARN radars. We are grateful to the many engineers and scientists who made the Cluster mission possible.

[24] Amitava Bhattacharjee thanks Raymond Greenwald and another reviewer for their assistance in evaluating this paper.

References

Avanov, L. A., V. N. Smirnov, J. H. Waite Jr., S. A. Fuselier, and O. L. Vaisberg (2001), High-latitude magnetic reconnection in sub-Alfvénic flow: Interball Tail observations on May 29, 1996, *J. Geophys. Res.*, *106*, 29,491.

Bavassano Cattaneo, M. B., et al. (2006), Kinetic signatures during a quasi-continuous lobe reconnection event: Cluster Ion Spectrometer (CIS) observations, *J. Geophys. Res.*, *111*, A09212, doi:10.1029/2006JA011623.

Chisham, G., M. P. Freeman, I. J. Coleman, M. Pinnock, M. R. Hairston, M. Lester, and G. Sofko (2004), Measuring the dayside reconnection rate during an interval of due northward interplanetary magnetic field, *Ann. Geophys.*, *22*, 4243–4258.

Cowley, S. W. H., and M. Lockwood (1992), Excitation and decay of solar wind-driven flows in the magnetosphere-ionosphere system, *Ann. Geophys.*, *10*, 103–115.

Crooker, N. U. (1979), Dayside merging and cusp geometry, *J. Geophys. Res.*, *84*, 84,951–84,959.

Crooker, N. U., and F. J. Rich (1993), Lobe cell convection as a summer phenomenon, *J. Geophys. Res.*, *98*, 13,403–13,407.

Dungey, J. W. (1963), The structure of the ionosphere, or adventures in velocity space, in Geophysics: The Earths Environment, edited by C. DeWitt, J. Hiebolt, and A. Lebeau, 526-536, Gordon and Breach, New York.

Eriksson, S., et al. (2005), On the generation of enhanced sunward convection and transpolar aurora in the high-latitude ionosphere by magnetic merging, *J. Geophys. Res.*, *110*, A11218, doi:10.1029/2005JA011149.

Fuselier, S. A., B. J. Anderson, and T. G. Onsager (1995), Particle signatures of magnetic topology at the magnetopause: AMPTE/CCE observations, *J. Geophys. Res.*, *100*, 11,805.

Fuselier, S. A., B. J. Anderson, and T. G. Onsager (1997), Electron and ion signatures of field line topology at the low-shear magnetopause, *J. Geophys. Res.*, *102*, 4847–4863.

Gosling, J. T., M. F. Thomsen, S. J. Bame, R. C. Elphic, and C. T. Russell (1991), Observations of reconnection of interplanetary and lobe magnetic field lines at the high-latitude magnetopause, *J. Geophys. Res.*, *96*, 14,097–14,106.

Gosling, J. T., M. F. Thomsen, G. Le, and C. T. Russell (1996), Observations of magnetic reconnection at the lobe magnetopause, *J. Geophys. Res.*, *101*, 24,765–24,774.

Greenwald, R. A., et al. (1995), DARN/SuperDARN: A global view of high-latitude convection, *Space Sci. Rev.*, *71*, 763–796.

Hardy, D. A., L. K. Schmitt, M. S. Gussenhoven, F. J. Marshall, H. C. Yeh, T. L. Schumaker, A. Huber, and J. Pantazis (1984), Precipitating electron and ion detectors (SSJ/4) for the block 5D/Flights 6-10 DMSP (Defense Meteorological Satellite Program) satellites: Calibration and data presentation, Rep. AFGL-TR-84-0317, Air Force Geophysics Laboratory, Hanscom AFB, Mass.

Imber, S. M., S. E. Milan, and B. Hubert (2006), The auroral and ionospheric flow signatures of dual lobe reconnection, *Ann. Geophys.*, *24*, 3115–3129.

Kessel, R. L., S.-H. Chen, J.-L. Green, et al. (1996), Evidence of high-latitude reconnection during northward IMF: Hawkeye observations, *Geophys. Res. Lett.*, *23*, 583.

Lavraud, B., M. F. Thomsen, B. Lefebvre, S. J. Schwartz, K. Seki, T. D. Phan, Y. L. Wang, A. Fazakerley, H. Rème, and A. Balogh (2006), Evidence for newly closed magnetosheath field lines at the dayside magnetopause under northward IMF, *J. Geophys. Res.*, *111*, A05211, doi:10.1029/2005JA011266.

Lockwood, M., and J. Moen (1999), Reconfiguration and closure of lobe flux by reconnection during northward Imf: Possible evidence for signatures in cusp/cleft auroral emissions, *Ann. Geophys.*, *17*, 996–1011.

Lockwood, M., and S. K. Morley (2004), A numerical model of the ionospheric signatures of time-varying magnetic reconnection: I. Ionospheric convection, *Ann. Geophys.*, *22*, 73–91.

Lockwood, M., B. S. Lanchester, S. K. Morley, K. Thorp, S. E. Milan, M. Lester, and H. Frey (2006), Modeling the observed proton aurora and ionospheric convection responses to changes in the IMF clock angle: 2. Persistence of ionospheric convection, *J. Geophys. Res.*, *111*, A02306, doi:10.1029/2003JA010307.

Mende, S. B., et al. (2000), Far ultraviolet imaging from the IMAGE spacecraft. 3. Spectral imaging of Lyman-alpha and OI 135.6 nm, *Space Sci. Rev.*, *91*, 287–318.

Milan, S. E., M. Lester, S. W. H. Cowley, K. Oksavik, M. Brittnacher, R. A. Greenwald, G. Sofko, and J.-P. Villain (2003), Variations in the polar cap area during two substorm cycles, *Ann. Geophys.*, *21*, 1121–1140.

Øieroset, M., J. Raeder, T. D. Phan, S. Wing, J. P. McFadden, W. Li, M. Fujimoto, H. Rème, and A. Balogh (2005), Global cooling and densification of the plasma sheet during an extended period of purely Northward IMF on October 22-24, 2003, *Geophys. Res. Lett.*, *32*, L12S07, doi:10.1029/2004GL021523.

Onsager, T. G., J. D. Scudder, M. Lockwood, and C. T. Russell (2001), Reconnection at the high-latitude magnetopause during northward interplanetary magnetic field conditions, *J. Geophys. Res.*, *106*, 25,467–25,488.

Phan, T.-D., et al. (2003), Simultaneous Cluster and IMAGE observations of cusp reconnection and auroral proton spot for northward IMF, *Geophys. Res. Lett.*, *30*(10), 1–16, 1509, doi:10.1029/2003GL016885.

Reiff, P. H., and J. L. Burch (1985), IMF By-dependent plasma flows and Birkeland currents in the dayside magnetosphere 2. A global model for northward and southward IMF, *J. Geophys. Res.*, *90*, 1595–1609.

Retinò, A., M. B. Bavassano Cattaneo, M. F. Marcucci, et al. (2005), Cluster multispacecraft observations at the high-latitude duskside magnetopause: implications for continuous and component magnetic reconnection, *Ann. Geophys.*, *23*, 461–473.

Retinò, A., A. M. Vaivads, M. André, et al. (2006), The structure of the separatrix region close to a magnetic reconnection X-line: Cluster observations, *Geophys. Res. Lett.*, *33*, L06101, doi:10.1029/2005GL024650.

Ruohoniemi, J. M., and K. B. Baker (1998), Large-scale imaging of high-latitude convection with Super Dual Auroral Radar Network HF radar observations, *J. Geophys. Res.*, *103*, 20,797–20,811.

Ruohoniemi, J. M., and R. A. Greenwald (2005), Dependencies of high-latitude plasma convection: Consideration of interplanetary magnetic field, seasonal, and universal time factors in statistical patterns, *J. Geophys. Res.*, *110*, A09204, doi:10.1029/2004JA010815.

Safrankova, J., Z. Nemecek, D. G. Sibeck, L. Prech, J. Merka, and O. Santolik (1998), Two-point observation of high-latitude reconnection, *Geophys. Res. Lett.*, *25*, 4301–4304.

Song, P., and C. T. Russell (1992), Model of the formation of the low-latitude boundary layer for strongly northward interplanetary magnetic field, *J. Geophys. Res.*, *97*, 1411–1420.

E. Amata, D. Ambrosino, M. B. Bavassano Cattaneo, I. Coco, and M. F. Marcucci, Istituto di Fisica dello Spazio Interplanetario-INAF, Roma, Italy. (federica.marcucci@ifsi-roma.inaf.it)

S. E. Milan, Departement of Physics and Astronomy, University of Leicester, Leicester, UK.

A. Retinò, Swedish Institute of Space Physics, Uppsala, Sweden.